Egypt. J. Chem. **Vol. 67** No. 10 pp. 109 - 125 (2024)

Egyptian Journal of Chemistry

http://ejchem.journals.ekb.eg/

Assessment of Antibacterial Fabric Nanocomposites Utilizing Polymer Blend and Silver/Copper Oxide after Irradiation with Electron Beam

H. M. Eyssa[1*], Rawia F. Sadek[2], R.M. Attia[1]

[1]*Radiation Chemistry Department, National Center for Radiation Research and Technology (NCRRT), Egyptian Atomic Energy Authority, Cairo, Egypt.*

[2]*Drug Radiation Research Department, National Center for Radiation Research and Technology (NCRRT), Egyptian Atomic Energy Authority, Cairo, Egypt.*

Abstract

There is no doubt that cotton textiles are fully qualified for medical uses, but they are a major source of bacterial growth and reproduction. Accordingly, the present study propose the use of ethylene glycol/carboxymethyl cellulose/polyethylene glycol hydrogel/silver/copper oxide nanocomposites (EG/CMC/PEG/Ag/CuO ratio (0.012, 0.5, 1 and 2%) and then subjecting them to the electron beam irradiation (at doses of 5, 10 and 25kGy). This results in getting rid of bacteria and reducing their severe effects of infections on the surfaces of textiles. The green synthesis of nano-CuO was conducted using the material extracted from the leaves of the *Moringa* plant, and then cotton samples were immersed in the sample. Transmission Electron Microscope (TEM) and X-ray diffraction (XRD) Techniques were used to prove the formation of CuO nanoparticles. The synergistic influence of CuO and Ag nanoparticles on the antibacterial activity, water vapor permeability (WVP%), mechanical, and thermal properties of the cured fabrics, CMC–PEG–EG composites, was studied. The current study concluded that the fabrics that were treated showed impressive results against bacteria with an inhibition area of twenty and fifteen mm for *E.coli* and *S.epidermis* bacteria, respectively.EG/CMC/PEG combined with $12x10^{-3}$% nano-CuO and 0.5% nano-CuO at doses of 5 and 25 kGy were the most effective composites. The present study also displayed that textiles containing EG/PEG/CMC/nano-CuO/Ag have a less WVP% estimated at 0.092($6x10^{-3}$%Ag/2.0% nano-CuO) at a dose of 5 kGy compared to unfilled textiles (0.35). of the electron radiation till 25 kGy led to significantly higher tensile strength, compared to unfilled and unirradiated fabrics. The thermal stability was enhanced by adding CuO nanoparticles up to 2%.

Keywords: Cotton textiles improvement, *Moringa plant*, Nanocomposites, A radiation of electron beam

Introduction

There is no doubt that the use of radiation and radioactivity is an interesting thing in daily life, according to many publications [1-99]. It has been noted in recent years that there is a great academic interest in the subject of many different textiles that have the ability to resist many microbes, such as different types of bacteria [100]. It is worth mentioning here to highlight the importance of cotton textiles because of their special nature unlike other textiles, but unfortunately that nature is a good source of a suitable environment for the growth of bacteria and fungi. Many organic nanoparticles have also been used, which have the ability to protect cotton textile products from microbes [101]. Both carboxymethyl cellulose (CMC) and polyethylene glycol (PEG) are used in the formulation of hydrogels which are biodegradable [102-106]. Studies have concluded that PEG is hydrophilic as well as hydrophobic [107]. In addition, the studies have shown that electron beam irradiation contains unsaturated monomers, complementary additives, as well as oligomers that are desired properties. Likewise, ethylene glycol (EG) is a hydrophilic monomer that improves flexibility and homogeneity [108]. Metal nanoparticles or oxides can be utilized as antimicrobial agents such as nano-Ag/CuO [109]. It is worth noting to demonstrate the importance of the

*Corresponding author e-mail: Hanan_eyssa@yahoo.com. (Hanan. M. Eyssa).
Receive Date: 27 December 2023, Revise Date: 14 February 2024, Accept Date: 15 April 2024
DOI: 10.21608/ejchem.2024.258271.9100

electron beam irradiation as an effective tool in treating, smoothing and tangling, it is also considered it a clean method [110]. Khafaja et al. [111], treated cotton fabrics using CMC-polyvinyl alcohol hydrogel-TiO_2 nanoparticles, with the use of gamma rays, proving their ability to resist a type of bacteria. The present study has been carried out on the same scale and antimicrobial resistance on cotton surfaces has been achieved which is consistent with the results found in a previous study [112], using a study of polyester with (vinyl alcohol)/plasticized starch (PVA/PLST) as well as nanocomposites such as (Cu/CS) as antimicrobials. *Moringa plant* (leaves) is considered a rich source of beta-carotene along with protein and many antioxidants; and thus improve the shelf life of fats within foods ascribed to the presence of various types of ascorbic acid, flavonoids, phenols, and carotenoids as antioxidants [113, 114]. In the current study, CuO NPs was prepared by green chemistry (sol-gel). *Moringa leaves* were treated as a potential reducing agent, to prepare PEG/CMC/EG/Ag that was used at a fixed percentage without change, but nano CuO was treated with several concentrations and its effect was evaluated by electron beam irradiation on the fabric, against the antimicrobial properties. Moreover, a big deal of work was done on the practical evaluation of the treated cotton fabrics in terms of their physical and thermal properties. Fourier transform infrared (FTIR) was used to prove the occurrence of crosslinking through cotton fabric, and an electron microscope was used to evaluate the size of CuO NPs (TEM).

Experimental

Chemicals

Plain-weave cotton fabrics were purchased from El-Nasr Company for Spinning, Weaving, and Dyeing, El-Mahalla El-Kubra, Egypt. The cotton fabrics were scoured and not subjected to any further finishing processes. Polyethylene glycol was purchased from Fluka Co., Germany, with an OH Functionality = 2.0, and Mw = 600 g/mol. CMC sodium salts of high viscosity were bought from El-Nasr Pharmaceutical Chemicals, Egypt.EG was obtained from Qualikems Fine Chem Pvt. Ltd., India, and $CuCl_2 \cdot 2H_2O$ (copper chloride dihydrate, 98.0%) was provided by LOBA Chemie Pvt. Ltd., China. Ethanol of laboratory grade was supplied by El-Nasr Pharmaceutical Chemicals, Egypt. Ag NPs were prepared according to a previous work [115]. *Moringa* leaves were collected from the Department of Botany, College for Women, Ain-Shams University, Cairo, Egypt. Laboratory-grade agar powder was obtained from Nice Chemicals, India. Pathogenic microorganisms of both gram-negative (*Escherichia coli*) and gram-positive (*Staphylococcus epidermis*) bacteria were obtained from Microbiologics, Inc., Minnesota, USA.

Extraction and preparation of *Moringa*

The leaves of *Moringa* were washed with tap of water followed by deionized water to get rid of any undesired materials. The leaves were dried at 37^0C to get ready for use. Then the extract, green *Moringa* (one gram) boiled utilizing deionized water for one hour. A filtration process was carried out by Whatman No one filter paper and then it was stored in cool medium. This extract was used for preparing CuO NPs.

Synthesis of nanoparticle (Copper oxide)

A sol gel process has been utilized to prepare a nanoparticle (CuO) using green chemistry, (Figure 1). The nanoparticle, copper oxide, has been mixed through deionized water with stirring and heating for preparing solution (0.2 M), then an aqueous extract *of Moringa* leaves has been added to a soln of nanoparticle. Followed by NaOH, eight molar, to the medium above till a black precipitate has been formed, as a large quantity. The final precipitate has been washed a lot of times utilizing, deionized water and has been filtered and then it was dried at a high, temperature (100°C). The precipitate faced calcination at five hundred °C for four hours.

Figure.1. Schematic diagram for the nano CuO preparation

Preparation of a nanocomposite (EG/CMC/PEG/Ag/CuO)

A nanocomposite (1.35g) was added with ethanol and deionized water then stirring for two hours at eighty °C till final miscibility was done. During continuous stirring, the perfect weight of CuO {12/1000, 5/10, one, and two %} with silver, {6/1000 %} with respect to the total volume, was put to the solution on the form of a dispersed phase realizing the composite.

Cotton fabric and electron beam (EB) irradiation application

Samples of cotton textiles were filled in the nanocomposites solutions in the perfect form compressed to get the aggregate to hundred percent, followed by irradiating at different doses. The cotton fabrics with different cases (unmodified and modified) were subjected to electron beam radiation at 37°C, with a 2.7 million electron volt and twenty five kW EB accelerator, at 10 mA and doses of irradiation of 5, 10, and 25 kGy.

The synthesized CuO NPs Characterization

A transmission electron microscopy (TEM) model JEM-2100 was used to measure the size of particle and the shape with a voltage of two hundred kilovolts of the nanoparticles. X-ray diffraction (XRD){6000, Shimadzu Instruments} was utilized to investigate the prepared nanoparticles. It has patterns from four to nighty degree at a scanning rate of two °/min on a diffractometer with Cu Kα radiation (mA current, and forty kV voltages) at 37ºC. In addition Energy dispersive X-ray (EDX) and mapping image analysis have been used to determine the mapping images and composition of the elements of the nanoparticles (CuO) which were examined by an EDX unit (Smart EDX Company, UK).

The treated cotton textiles characterization

Morphological analysis

The scanning electron microscope (SEM) (ZEISS EVO 15 SEM, UK) was used to characterize the nanoparticles as powder beside the fracture morphology, M (0.012, 1/2, 1.0, with 2.0% nano CuO) on the surface of cotton textiles.

Fourier transform infrared spectroscopy

The nanocomposites were examined by FTIR spectrometer (Vertex 70 Bruker Optics, Germany) that has a resolution of four cm^{-1} to software sixty four scans with within a wide λ range 400–4000 cm^{-1} at 37ºC.

Measurements of mechanical behaviour

The mechanical behavior was examined at 37°C ± 2°C according to ASTM D5034. Quadrangular specimens dimensions of fifty multiply hundred mm have been detected. Elongation at break and tensile strength have been detected at a crosshead speed of seventy mm/minute on a Qchida computerized machine. The tested mechanical parameters (average value) was determined though three samples examined, at least.

The permeability of water vapor, WVP

WVP was measured according to the AS-2001.2.34:1990 (standard). The test of the prepared sample (cotton fiber) has been made at 37°C for twenty four hour. Then it was elevated at seventy°C for two hours. Using a pressure of 100 kPa, tube no-04 (L/min) and a minor opening (d. of 2.8 cm) for many times.

Thermogravimetric analysis measurements

The sample (modified cotton fabrics) was examined by thermogravimetric analysis using a TGA-fifty (Shimadzu, Japan) at 10°C/minutes using a gas (nitrogen) and temperature from 37°C to six hundred, and 20 mL/min as flow rate to detect the thermal stability. In addition, the specimen weights have been in the range from two to five mg.

The antibacterial activity of the coated textiles detection

Antimicrobial arbitrary agar diffusion way

A disk diffusion test was prepared typically according to the method of Selvarani et al. [116], in which the antimicrobial activity of the tested nanocomposites was studied and different types of the bacterial activity gram-positive (*Staphylococcus epidermis*) and gram-negative (*Escherichia coli*) were identified.

RESULTS AND DISCUSSION

The synthesized nano CuO estimation

XRD was used to prove the structure of the nano CuO, as shown in Figure (2). It has become clear that there are two peaks; the highest of 2θ are 35.62º and 38.7º, which correspond to (002) and (111). It has become clear that nano CuO has a structure of monoclinic card no.45-0937, and the sharp and high peaks indicate that the product was prepared with a superior crystallinity [117, 118].

Both TEM and SEM images as (Figure 3) are used to reveal that the prepared nanoparticles, nano CuO are homogeneous and spherical according to [117, 119]. The microscopic image (TEM) also showed the average diameter of the nano CuO, which is approximately 7-18 nm (Fig. 3a). However, Figure (3b) has shown the nanostructure of the prepared nanoparticles, nano CuO which is consistent with the image given by the SEM [120], which also shows the morphology of the prepared nanoparticles with a spherical shape. EDX was used to examine the components of the prepared nanoparticles in order to determine the proportion of each element (copper and oxygen) as shown in Figure (4a). Figure (4a) shows that only copper and oxygen are present, which indicates that the prepared sample is completely pure. The percentages of these elements (copper and oxygen) are 55.94% and 44.06%, respectively. Figure (4b) also presents the racial maps. Based on the abovementioned, it could be concluded that this nanocomposite contains oxygen and copper, and this is consistent with the aforementioned analyses

results, (EDX). In addition, element determination images showed a uniform dispersion of oxygen and copper with a high purity.

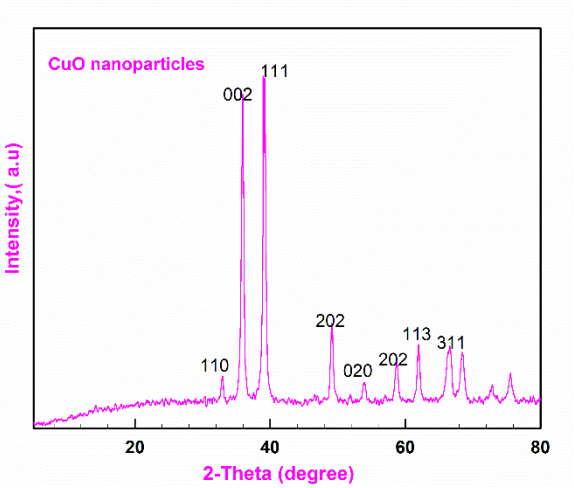

Figure.2. XRD pattern of nano CuO synthesized

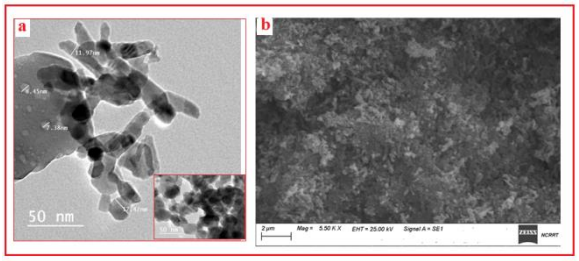

Figure 3. (a) TEM, (b) SEM images of nano CuO synthesized

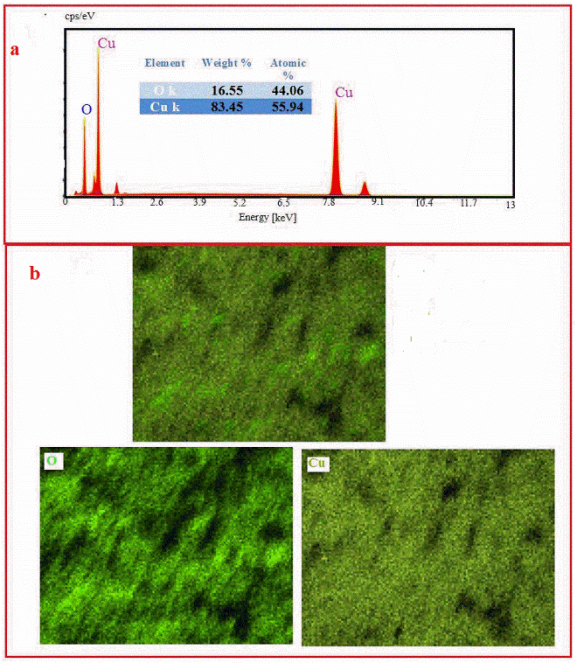

Figure 4. (a) EDX analysis and (b) mapping images of nano CuO synthesized

Modified cotton fabric nanocomposites measurements

In addition, a good chemical crosslinking bonds have been formed between PEG with CMC in the presence of carboxyl groups of CMC, and EG monomer with incorporating different nano CuO ratios with continuous stirring and heating were followed by electron beam radiation as seen in Figure (5).

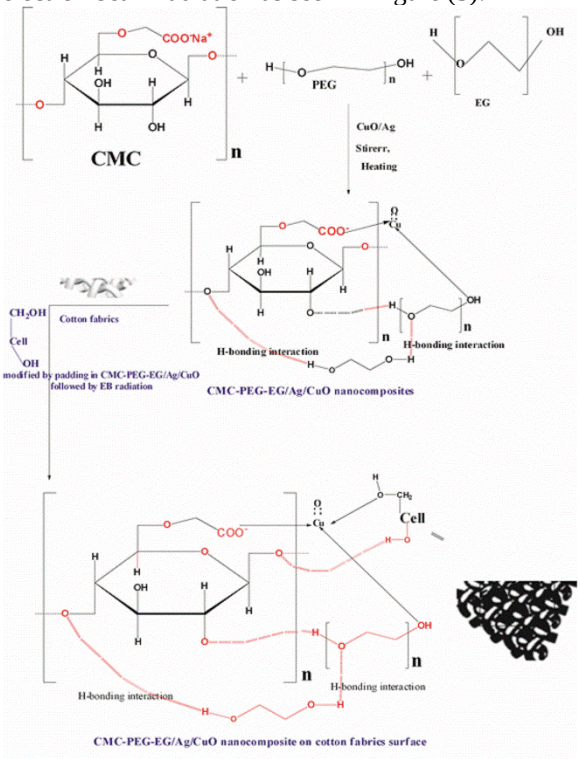

Figure.5. Schematic diagram of the compatibilizing mechanism of Ag/CuO NPs within the CMC/PEG/EG hydrogel on surface of cotton fabrics

FTIR spectroscopy analysis

To study the chemical reactions that took place into the polymer utilized, FTIR technique elucidated the influence of nano copper oxide on the Ag/EG/CMC/PEG. Figure (6) clarifies the FTIR spectra of the irradiated cotton textiles (control), the surface of treated cotton textile by EG/CMC/PEG, and the treated cotton textile utilizing Ag/EG/CMC/PEG filled by various ratios of nano copper oxide. The FTIR spectrum elucidated the peaks of characteristic of the cotton textiles (control) at 3424, and 2898 cm^{-1}, owing to the vibrations of stretching −OH, and stretching of aliphatic CH, respectively, whilst (C–O–C) stretching of asymmetric bridge was ascribed to 1035 cm^{-1} of the main peaks of the cellulose structure. The peak around 1603 cm^{-1} was noticed for vibrations of bending (OH) of the cellulose molecular. The IR spectrum of EG/PEG/CMC on the surface of the cotton textile demonstrated the function groups related to PEG, CMC and EG polymers. The

spectrum of EG/PEG/CMC hydrogel showed a main peak at 3277 cm^{-1} owing to inter-molecular H-bonding [121, 88]; 2890 cm^{-1} was referred to a CH_2 stretching and 1715 cm^{-1} to (C=O) stretching. An anti-symmetrical vibration of the ionized COO^- group appeared at the band 1595 cm^{-1} [122], the peak of the scissoring bending vibration of CH_2 was noticed around 1420 cm^{-1}, and the vibration of bending of CH was observed at 1325 cm^{-1}[123]. The band located about 1022 cm^{-1} was associated with O-C of the vibration of stretching of the cellulose structure [124], while the band assigned to 1250 cm^{-1} was ascribed to alcohol (O-C). Hence, the results proposed that CMC/PEG/EG presented on the surface of the cotton fabric led to the interpenetrating polymer network formation of EG/CMC/PEG on the cotton textile. After adding various nano CuO ratios with Ag/EG/PEG/CMC, the low or high peaks of intensity were seen in the FTIR spectrum of the nanocomposite owing to the peak position change. The same band appeared at approximately 556 cm^{-1} of Ag/EG/CMC/PEG/(12x10^{-3}% and 1/2% nano CuO), whilst the peak at 497 cm^{-1} was attributed to the Ag/EGCMC/PEG/(2.0 % nano CuO). The peak position and change in intensity indicated that the nano CuO and CMC/PEG/EG/Ag matrix interacted [125]. Meanwhile, the peak appearing between 400 and 600 cm^{-1} may reflect the O-Cu [126]. For the filled samples (Ag/EG/CMC/PEG) with various nano CuO ratios, the absorption band appeared at 3330, 2897, 1712, 1606, 1420, 1327, 1248, and 1021 cm^{-1}, which is attributable to the (–OH) stretching, (C–H) vibration of stretching, (C=O) vibration of stretching, (COO–) antisymmetrical vibration, the scissoring bending vibration of CH_2, bending vibration of CH, C–O (alcohol), and C–O stretching vibration, respectively.

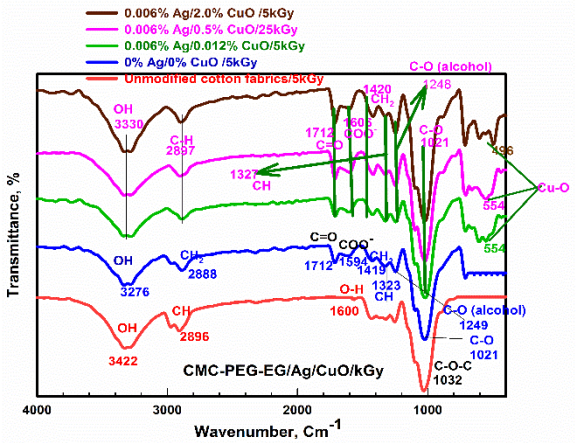

Figure 6. Fourier transform infrared spectra of untreated cotton fabrics at 5 kGy**,** fabrics by immersing in EG/CMC/PEG at 5 kGy, fabrics by immersing in EG/CMC/PEG containing Ag(0.006%)/nanoCuO (0.012%) at 5 kGy, fabrics by immersing in EG/CMC/PEG containing Ag (0.006%)/nano CuO (1/2%) at 25 kGy and fabrics by immersing in EG/CMC/PEG containing Ag (0.006%) Ag/ nano CuO (2%) at 5 kGy

Morphology analysis by SEM

Figure (7) shows the sample loaded on the nanocomposites prepared at the optimum values such as nanoparticles (12x10^{-3}%, 1/2%, 1.0%, and 2.0%) under irradiation doses of 5 and 25 kGy. Samples that have the ability to outperform different types of bacteria were also chosen. This is shown in Figure (7a), an image with smooth, homogeneous structures as well as an ideal distribution of 0.012% nano CuO for the nanocomposites surface of the cotton sample. Comparing Figure (7b) with Figure (7a) in, it is clear that the nanocomposites concentration prepared at 0.5% has an ideal homogeneous and cohesive structure with a homogeneous and equal distribution with the surface of the cotton sample, in addition to the fact that there is an intense reaction between the molecules nano copper oxide and the Ag/EG/PEG/CMC chains. A coordination bond occurred between the carboxyl group present (CMC) with the copper ion according to a previous publication [127], as well as a covalent bond with the sample through an esterification reaction upon heating and radiation. By increasing the nano CuO concentration from 1% to 2%, there were few clusters of small nano CuO particles on the sample tissue (Figure 7c-7d). This leads to an intense interaction between the different particles.

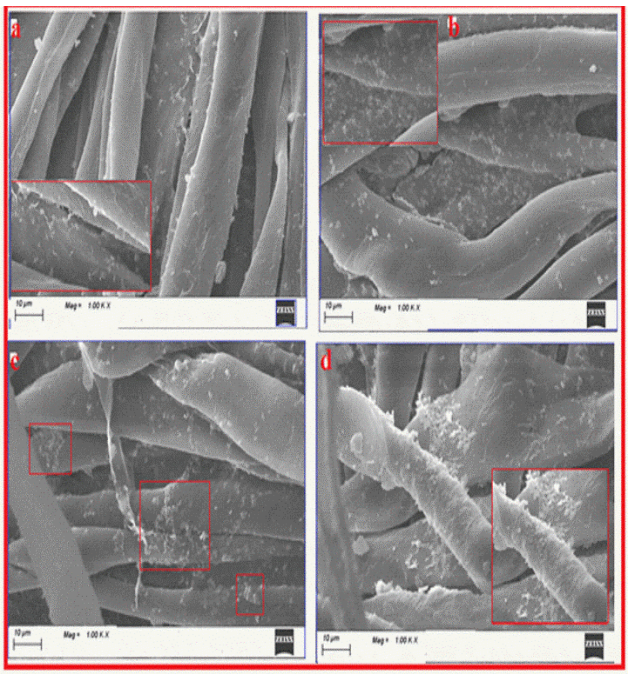

Figure 7. Scanning electron micrographs of treated cotton fabrics by EG/CMC/PEG/Ag with various concentrations of nano CuO: (a) irradiated EG/CMC/PEG/Ag (0.006%) / (12x10^{-3}%) nano CuO, (b) irradiated EG/CMC/PEG/Ag (0.006%) / (1/2%) nano CuO, (c) EG/CMC/PEG/Ag (0.006%) / (1%) nano CuO and (d) irradiated EG/CMC/PEG/Ag (0.006%) / (2%) nano CuO

Mechanical property

The stress-strain diagram is the basis for mechanical parameter applications. Both of Figs. (8&9) indicate the effective of irradiation dose and the various ratios of nano CuO on the elongation at break (Eb) and tensile strength (TS) of fabrics sample immersed with nano CuO and CMC/PEG/EG/Ag hydrogels.

It was noted that TS depended basically on the radiation doses.

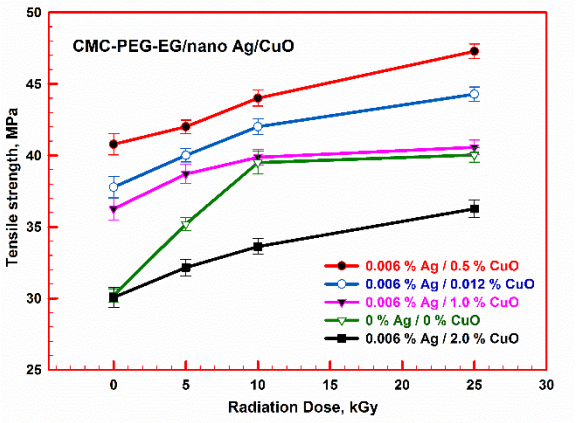

Figure 8. The tensile strength of cotton fabrics by immersing in EG/CMC/PEG, and cotton fabrics by immersing in EG/CMC/PEG containing Ag (0.006%)/ various concentrations of nano CuO at different radiation doses

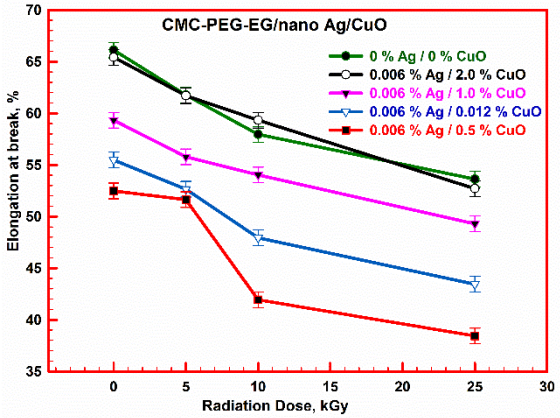

Figure 9. The elongation at break of cotton fabrics by immersing in EG/CMC/PEG, and cotton fabrics by immersing in EG/CMC/PEG containing Ag (0.006%)/ various concentrations of nano CuO at different radiation doses

The TS of the modified and unmodified samples, cotton textiles progressively elevated by increasing the amount of irradiation to a dosage of 25kGy. The incline in (TS) values up to 25kGy could be ascribed to the crosslinking density of the nanocomposites in the sample. It is worth noting here that the (TS) values increased by using 25kGy due to the presence of dense crosslinking on the surface of the sample. The optimum values of the stress (for irradiated and unirradiated samples of nanocomposites at 25kGy at 0.5% copper oxide) were (74%) and (86%), respectively. However, the values of TS elevated by the incorporation of nano CuO till (1/2%) for different samples (unirradiated and irradiated) wrapped by CuO/Ag/EG/CMC/PEG hydrogel. The elevation of the TS rate may be because of the symmetrical allocation of nano CuO in the CMC/PEG/EG that reinforced the interfacial adhesion and lamb transmit among the EG/PEG/CMC and nano CuO. It is possible that the increase in the network structure is due to the presence of nano CuO, which in turn causes the H-bonding formation through the different polar groups between them and allows the potential adhesion formation (coordinate bonds) between EG/PEG/CMC and Cu^{-} [127], thus resulting in an increment in the (TS) of CuO/Ag/EG/PEG/CMC nanocomposite. The reduced values of TS for the highest nano CuO ratio (one and two %) have been ascribed to nano CuO-nano CuO cluster, causing a low interfacial interaction with polymer blend. The high reactivity of nano CuO causes a cluster that reduces their features. The (TS) of the modified textiles, cotton was also found to be higher than others were. This may be because of the small layer of composites that resist tension surrounding the sample. It was also observed that there are similar trends with the elongation. It is important here to emphasize that the mechanical properties mainly depend on dispersion as well as interfacial interactions between the polymer chains (CMC/PEG/EG) on the surface of the fabrics [128].

The permeability of water vapor of cotton sample (modified cotton fabrics)

WVP is considered constant under any conditions. It is worth noting here that materials that love water (hydrophilic) are different from this ideal performance due to the attachment of water to the polar groups of the film structures [129]. The permeability of water vapor (WVP) is a critical factor to be discussed. At the beginning, the pervading particles abbreviate on superficial and solubilize addicted on the surface of the film. It is shaded through dispersion as the injected molecules must negotiate their way during the film. At the end, these molecules neglect to forfeiture the film surface at another direction. Both modified and unmodified cotton textiles are considered the same. It can be identified that the steam has been dispersed by the absence of any open holes [130]. However, after the treatment of cotton textiles by Ag/EG/PEG/CMC composite with various ratios of nano CuO and a fixed radiation dose (5kGy), it resulted in the water vapor resistance being completely changed. This was indicated in Tab. (1) that the permeability of water vapor of the unmodified sample notably elevated than

the modified one, sample cotton fabrics. This prevents the transfer of moisture through the pores, while providing strong resistance to water vapor on the modified cotton fabrics sample. This is ascribed to the nano CuO which has less permeability of water vapor [117, 125]. It is possible that the low permeability of water vapor amounts in the sample modified to the hydrophobic nature of nano CuO. There is also a coordination interaction that may occur between nano CuO and hydroxyl groups present in polymer chains in the sample prepared through the coordinate or hydrogen bonds formation. These bonds could produce more crosslinking in the entire matrix suit. This leads to reducing the dispersion caused by water vapors through the films.

Table 1. Water vapor permeability for untreated and treated cotton textiles with Ag/different ratios of nano CuO crosslinked with EB radiation at 5 kGy.

Sample	Dose, kGy	Water vapor permeability %
Untreated cotton textiles	5	0.35± 0.1596
Treated cotton textiles with EG/CMC/PEG	5	0.25± 0.1596
Treated cotton textiles with EG/CMC/PEG /Ag 6x10^{-3}% /nano CuO 12x10^{-3}%	5	0.13± 0.1259
Treated cotton textiles with EG/CMC/PEG/Ag 6x10^{-3}% / CuO 1/2%	5	0.12± 0.1259
Treated cotton textiles with EG/CMC/PEG/Ag 6x10^{-3}% /nano CuO 1.0%	5	0.10± 0.1259
Treated cotton textiles with EG/CMC/PEG/Ag 6x10^{-3}% /nano CuO 2.0%	5	0.092± 0.1200

Thermal analysis

The untreated cotton textiles, the treated cotton textiles with immersing in composite EG/CMC/PEG and those immersed with Ag/EG/CMC/PEG by filling in various nano CuO concentrations and crosslinked by electron beam irradiation to different doses 5 and 25kGy Fig. (10). The thermogravimetric analysis, TGA indicated a main degradation state with the temperature range from 272°C to 326°C for all samples. Besides, it was found that the all-fabrics thermal stability, whether with immersing or not to be still constant at ~272°C. Additionally, the treated cotton with the EG/CMC/PEG and Ag/EG/CMC/PEG utilizing nano CuO concentrations 0.12%, 0.5%, and 2% exhibited comparatively elevated thermally stable state than the untreated sample. The derivative wt facing each other indicated identical trends; however, the reaction rate temp (T_{max}) for thermal degeneration (TD) was different from one substance to another (Fig. 10 and Tab. 2). Both of Fig. 10 and Tab. 2 indicated that:

Firstly; the untreated cotton textiles, the treated cotton textiles with immersing in composite EG/CMC/PEG and those immersed with Ag/EG/CMC/PEG by filling in various nano CuO concentrations and crosslinked by electron beam irradiation showed TD at 2 T_{max} of TD interaction rate owing to the presence of the hybrid structures of fabric [112].

Secondly, the treated cotton by EG/CMC/PEG composite and those treated by Ag/EG/CMC/PEG/ various nano CuO concentrations demonstrated remarkable enhancements in being thermally stable with elevated values of T_{max} more than the other sample (untreated). This can be owing to the occurrence of crosslinking bonds, chemically formed occurred among cellulose of fabric and Ag/CMC/PEG/EG/nano CuO using electron beam radiation [130]. It has been shown that the highest improvement of thermal stability is in the case of the first and second T_{max}, as well as in the case of the treated textile through various nano CuO content/ Ag/CMC/PEG/EG/. It was shown that the thermally stable nanocomposites on sample surface (modified) elevated with incorporating nano CuO. This could be under the influence of the formation of the positive structure of copper [125].

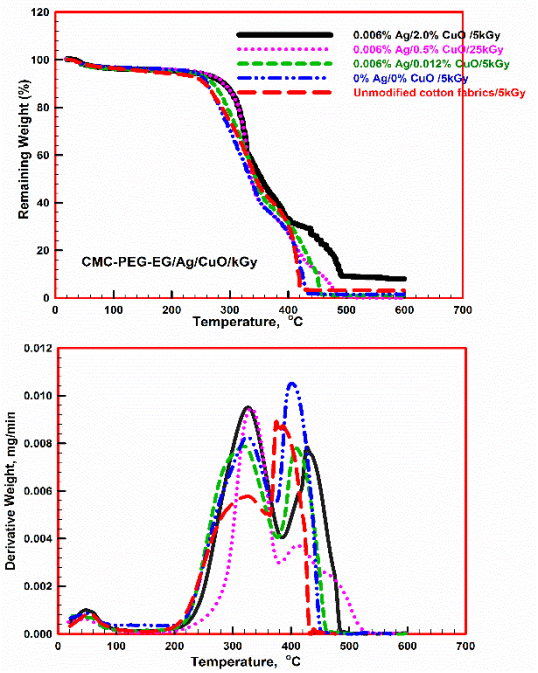

Figure. 10. Thermogravimetric analysis and the corresponding rate of thermal decomposition of untreated cotton fabrics at 5 kGy**,** fabrics by immersing in EG/CMC/PEG at 5 kGy, fabrics by immersing in EG/CMC/PEG containing Ag(0.006%)/nanoCuO (0.012%) at 5 kGy, fabrics by immersing in EG/CMC/PEG containing Ag (0.006%)/nano CuO (1/2%) at 25 kGy and fabrics by immersing in EG/CMC/PEG containing Ag (0.006%) Ag/ nano CuO (2%) at 5 kGy

Table 2. Temperatures of the maximum rate of reaction T_{max} (°C) of thermal degradation of untreated cotton textiles, treated cotton textiles /EG/ CMC/PEG, treated cotton textiles with EG/CMC/PEG/6x10^{-3} Ag/12x10^{-3} % nano CuO, treated cotton textiles with EG/CMC/PEG/6x10^{-3} Ag /1/2 % nano CuO and treated cotton textiles with EG/CMC/PEG/6x10^{-3} Ag /2.0 % nano CuO . The irradiation dose was at 5 and 25kGy.

Samples	Dose, kGy	1st T_{max} (°C)	2nd T_{max} (°C)
Untreated cotton fabrics	5	321	381
Treated cotton textiles with EG/CMC/PEG	5	324	404
Treated cotton textiles with EG/CMC/PEG /Ag 6x10^{-3}% /nano CuO 12x10^{-3}%	5	325	414
Treated cotton textiles with EG/CMC/PEG /Ag 6x10^{-3}% /nano CuO 1/2%	25	327	422
Treated cotton textiles with EG/CMC/PEG /Ag 6x10^{-3}% /nano CuO 2.0%	5	328	430

Antimicrobial activity of sample (modified)

Bacterial culture evaluation by examination

It is known that bacterial growth occure in various forms on cotton fabrics in particular may cause many problems, including unwanted odors and a change in colors, and this may lead to many health problems. Based on this, scientists have worked hard to solve these problems for cotton and other fabrics by using some metals that have the ability to deal with microbes in general, such as zinc, copper, gold, silver, and others. However, there is no ideal way to know the mechanism of action of mineral NPs to get rid of various bacterial microbes.

It is worth mentioning here the attempt to understand this mechanism [132]. It is assumed that the mineral NPs may be attached to the bacterial cell wall, which leads to the death of the bacteria by preventing the formation of the holes that form it, which helps in its reproduction. The antimicrobial characteristics of the untreated and treated cotton fabrics have been examined by the reaction of Ag/CMC/PEG/EG with different nano CuO ratios and EB radiation at various doses against Gram-positive or negative bacteria such as *S. epidermis (I)* or *E. coli (II)*, respectively. It was determined by the inhibition zone (mm) (Figs. eleven, twelve, & thirteen and Tab. 3) and accordingly the following was observed: The unmodified samples (US) showed no zones of inhibition against bacterial growth at all doses while, we found a small zone of inhibition for 5kGy. We infer from this those unmodified fabrics are unable to resist microbes. Certainly, it can be said that fabrics treated with (MS)/ polymer blend by incorporating nano CuO/Ag gave high efficiency against bacterial microbes under any dose that was used. Adding nano CuO ratio up to (1/2 %) caused the modified sample to have various types of antibacterial and antimicrobial properties for all doses compared to the unmodified cotton sample. It is also worth noting that when small ratios of nano CuO (12x10^{-3} and 1/2 %) were embedded in the modified sample, it gave higher features than the previous one. At the 5 and 25 kGy doses, respectively; the zones of inhibition were fifteen and twenty mm for bacteria *(I)* and *(II)*, respectively (including 12x10^{-3} and 1/2 % of nano CuO). It was observed that the inhibition zone slightly decreased with the increase in the ratio of nano CuO (one %) and the inhibition zone increases again by increasing the concentration of nano CuO (two %) at the irradiation dose of 5kGy, where it was twenty mm for bacteria *(I)* and fifteen mm for bacteria *(II)*. It was found that 5kGy of radiation had a higher ability to eliminate different bacterial microbes for various modified and unmodified samples *(I, II)* by appending Ag/nano CuO at various concentrations (12x10^{-3}, one, and two%), meanwhile 25kGy possessed a higher antibacterial characteristic of 1/2 % nano CuO. The antibacterial characteristic of fabrics treated with Ag/nano CuO at various contents depending on nanocomposite versus *(I)* and *(II)* should be studied according to factors. These include the metal/nano/polymer composites way which could be related to a synergistic influence among silver and nano CuO in the polymer that increases the antimicrobial impact of the nanocomposites comparing with nanoparticles alone [133]**.** It has been observed that at a low dose of the electron beam, up to 5kGy, a severe reaction occurs against both bacteria *(II)* and *(I)*. The reason for this may be that the polymers have a high ability to release over a long period of time, which makes it possible that the antibacterial action of nanocomposite may also be prolonged [134] as well as the severe surface area effect associated with the distribution of Ag NPs and copper oxide in the polymer.

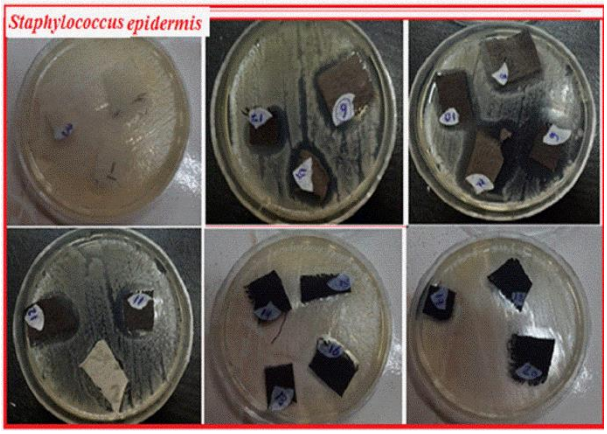

Figure 11. The antibacterial properties of the untreated and treated cotton fabrics by EG/CMC/PEG/Ag with various concentrations of nano CuO: for code samples (1, 2, 3 and 4) of the untreated cotton fabrics /EG/CMC/PEG, (5, 6, 7 and 8) of the treated fabrics by EG/CMC/PEG/Ag (0.006%)/ ($12x10^{-3}$%) nano CuO, (9, 10, 11 and 12) of the treated fabrics by EG/CMC/PEG/Ag (0.006%)/ (1/2%) nano CuO, (13, 14, 15 and 16) of the treated fabrics by EG/CMC/PEG/Ag (0.006%)/ (1.0%) nano CuO, and (17, 18, 19 and 20) of the treated fabrics by EG/CMC/PEG/Ag (0.006%)/ (2.0%) nano CuO at different radiation doses against (Gram +ve) Bacteria

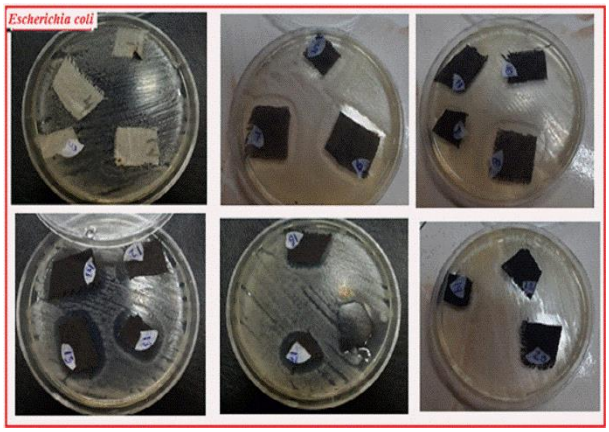

Figure 12. The antibacterial properties of the untreated and treated cotton fabrics by EG/CMC/PEG/Ag with various concentrations of nano CuO: for code samples (1, 2, 3 and 4) of the untreated cotton fabrics /EG/CMC/PEG, (5, 6, 7 and 8) of the treated fabrics by EG/CMC/PEG/Ag (0.006%)/ ($12x10^{-3}$%) nano CuO, (9, 10, 11 and 12) of the treated fabrics by EG/CMC/PEG/Ag (0.006%)/ (1/2%) nano CuO, (13, 14, 15 and 16) of the treated fabrics by EG/CMC/PEG/Ag (0.006%)/ (1.0%) nano CuO, and (17, 18, 19 and 20) of the treated fabrics by EG/CMC/PEG/Ag (0.006%)/ (2.0%) nano CuO at different radiation doses against (Gram –ve) Bacteria

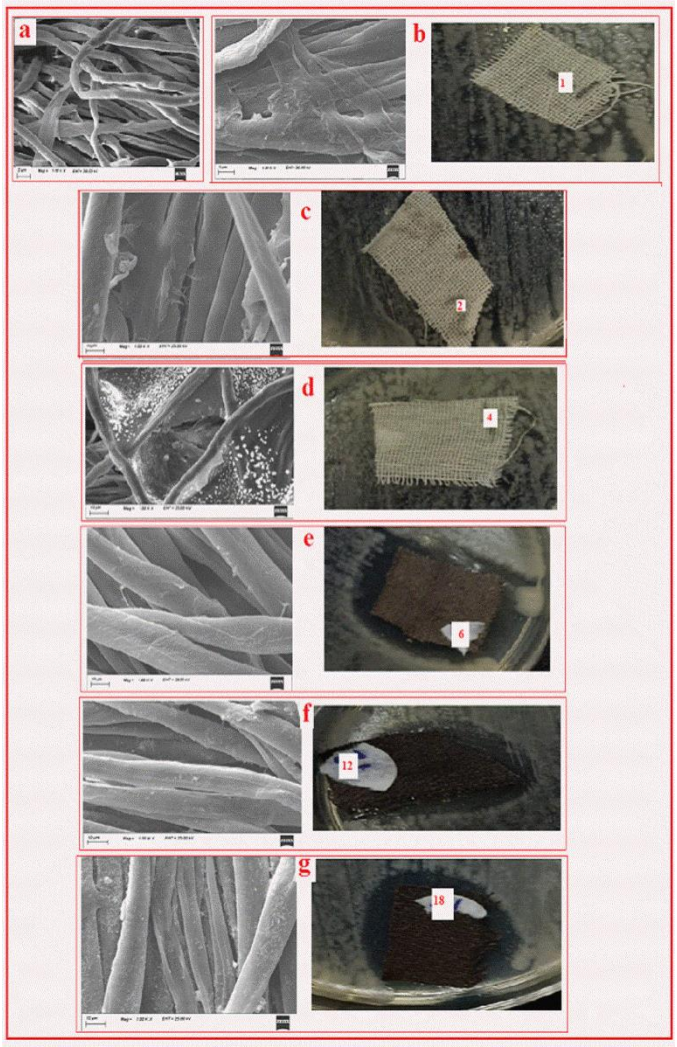

Figure 13. SEM images and dishes of cotton fabrics untreated and treated against bacteria: (A) pure cotton fabrics without bacteria, (B) fabrics by immersing in EG/CMC/PEG at 0 kGy, (C) fabrics by immersing in CMC/PEG/EG at 5 kGy, (D) fabrics by immersing in EG/CMC/PEG at 25 kGy, (E) fabrics by immersing in EG/CMC/PEG/Ag (0.006%)/ ($12x10^{-3}$%) nano CuO at 5 kGy, (F) fabrics by padding in EG/CMC/PEG/Ag (0.006%)/ (1/2%) nano CuO at 25 kGy and (G) fabrics by immersing in EG/CMC/PEG/Ag (0.006%)/ (2.0%) nano CuO at 5 kGy

Table 3. Inhibition zone of untreated and treated cotton textiles with various ratios of nano CuO for gram-positive and gram-negative with EB radiation**.**

Code sample	Conc of Ag/CuO %	Radiation dose, kGy	Inhibition zone(mm)	
			gram-positive (*Staphylococcus epidermis*)	gram-negative (*Escherichia coli*)
1	0/0	0	0 ± 0.0	0± 0.0
2	0/0	5	8 ± 0.7600	8± 0.7600
3	0/0	10	0 ± 0.0	0± 0.0
4	0/0	25	0 ± 0.0	0± 0.0
5	0.006/0.012	0	10 ± 0.1259	12± 0.1259
6	0.006/0.012	5	15 ± 0.2259	20± 0.1599
7	0.006/0.012	10	10 ± 0.2259	20± 0.1259
8	0.006/0.012	25	15 ± 0.7600	20± 0.2259
9	0.006/0.5	0	20 ± 0.5000	9± 0.5000
10	0.006/0.5	5	10 ± 0.2155	15 ± 0.1596
11	0.006/0.5	10	17 ± 0.2155	10± 0.2359
12	0.006/0.5	25	15 ± 0.1596	20± 0.2155
13	0.006/1	0	20 ± 0.2359	10.05± 0.3650
14	0.006/1	5	9 ± 0.1259	14± 0.2359
15	0.006/1	10	9 ± 0.1596	15± 0.2359
16	0.006/1	25	11 ± 0.2359	9± 0.7600
17	0.006/2	0	10 ± 0.3650	10± 0.5000
18	0.006/2	5	20 ± 0.2356	15± 0.2359
19	0.006/2	10	10 ± 0.2356	16± 0.2356
20	0.006/2	25	10 ± 0.1599	13± 0.3650

CONCLUSIONS

It is worth noting here that cotton textiles under the influence of bacterial microbes, change all their properties, such as smell, color, and so on. Accordingly, these (cotton) fabrics have been subjected to biomedical applications. There is no doubt that the green chemistry application with nanocomposites have contributed to obtaining cotton textiles free of all the defects mentioned above. The present study concludes that small-scale nano CuO is synthesized using *Moringa* plant extract, which acts as a reducing agent. The following factors were found from the treated samples containing this nanocomposite Ag/CuO/CMC/PEG/EG: The modified sample (cotton fabrics) showed much more immovability for *(II)* and *(I)* bacteria at all nano CuO concentrations ($12x10^{-3}$, 1/2, and two%)**,** $12x10^{-3}$ is the representative of the best utilized ratio in agreement with cost and antimicrobial effect. It has been observed that a marked improvement occurred in the mechanical characteristics of sample (MS) after Ag/concentrations nano CuO/MC/PEG/EG composite treatment up to 1/2 % nano CuO and 25kGy. The modified sample, fabrics with Ag/concentrations nano CuO/MC/PEG/EG composite exhibited increase in the stress values and elongation at break of the irradiated samples at 25kGy of the formulations of cotton textile nanocomposite at 0.5% nano CuO which were eighty six% and seventy two%, respectively.

Acknowledgement
The authors would like to thank the NCRRT, Egyptian Atomic Energy Authority, Cairo, Egypt for supporting the performance of the measurement of the present study.

Conflict of Interest
There is no conflict of interest related to this publication.

Funding
No author acquired any type of financial support for the achievement of this study or publication of the article by any funding agency.

Data Availability Statement
All the results were realized at Egyptian Atomic Energy Authority.

REFERENCES

[1] Sanad, M. H., Alhussein A. I. Preparation and biological evaluation of ^{99m}Tc N-histamine as a model for brain imaging: in silico study and preclinical evaluation. Radiochim. Acta, 106, 229-238 (2018).

[2] Sanad, M. H., Farouk, N., Fouzy, A. S. M. Radiocomplexation and bioevaluation of ^{99m}Tc nitrido-piracetam as a model for brain imaging. Radiochimic. Acta, 105(9), 729-737 (2017).

[3] Sanad, M. H., Rizvi, S. F. A., Farag, A. B. Synthesis, characterization, and bioevaluation of 99mTc nitrido-oxiracetam as a brain imaging model. Radiochimic. Acta, 109(6), 477-483 (2021).

[4] Sanad, M. H., Marzook, F. A., Ibrahim, I. T., et al., Preparation and Bioevaluation of Radioiodinated Omberacetamas a Radiotracer for Brain Imaging. J. Radiochemistry, 65, 114 – 121 (2023).

[5] Sanad, M. H., Marzook, F. A., Challan, .S. B., et al., Radioiodination, and Biological Assessment of Olsalazine, as a Highly Selective Radiotracer for Ulcerative Colitis Imaging in Mice. Arab. J. Nucl. Sci. &Applic, 56, 105 – 120 (2023).

[6] El-Kawy O., Sanad M. H., Marzook, F. A. ^{99m}Tc-Mesalamine as potential agent for diagnosis and monitoring of ulcerative colitis: labelling, characterization and biological evaluation. J.Radioanal. Nucl. Chem, 308 (1), 279-286 (2016).

[7] Sanad, M. H., Talaat, H. M., Fouzy, A. S. M. Radioiodination and biological evaluation of mesalamine as a tracer for ulcerative colitis imaging. Radiochimic. Acta, 106(5), 393-400 (2018).

[8] Sanad, M. H., Challan, S. B., Essam, H. M., Massoud, A. Assessment of Radiolabeled L-Carnitine for Hepatotoxicity Imaging in Rats. Radiochemistry, 65(1), 101–113 (2023).

[9] Sanad, M. H., Eyssa, H.M., Marzook, F. A. et al., Pharm. Chem. J, 57(4), 543 – 549 (2023).

[10] Sanad, M. H., Gomaa, N.M., El Bakary, N.M., Marzook, F. A., Sabry, A.B. Radioiodination and Biological Evaluation of Novel Quinoline Derivative for Infective Inflammation Diagnosis. Pharm. Chem. J, 57(7), 1–11 (2023).

[11] Sanad M.H., Eyssa H.M., Marzook, F.A., Farag, AB., Rizvi, S.F.A., Mandal, S.K. Comparative bioevaluation and ^{99m}Tc-Sn (II) lansoprazole as a model for peptic ulcer localization. Radiochemistry. 63(5), 642-650 (2021).

[12] Challan, S. B., Khater, S.I., Rashad, A.M. Preparation, molecular modeling and in-vivo evaluation of 99mTc-Oseltamivir as a tumor diagnostic agent. Int. J. Radiat. Res, 20(3), 635-642 (2022).

[13] Ibrahim, I. T., Sanad, M. H. Radiolabeling and biological evaluation of losartan as a possible cardiac imaging agent J. Radiochemistry, 55, 336-340 (2013).

[14] Sanad M. H, Ibrahim I.T. Radiodiagnosis of peptic ulcer with technetium-^{99m} pantoprazole. Radiochemistry, 55, 341-345 (2013).

[15] Sanad, M. H., Amin, A. M. Optimization of labeling conditions and bioevalution of ^{99m}Tc-meloxicam for inflammation imaging. J. Radiochemistry, 55, 521-526 (2013).

[16] Sanad, M. H., El-Tawoosy, M. Labeling of ursodeoxycholic acid with technetium-^{99m} for hepatobiliary imaging. J. Radioanal. Nucl. Chem, 298, 1105-1109 (2013).

[17] Amin, A. M., Sanad, M. H., Abd-Elhaliem, S. M. Radiochemical and biological characterization of ^{99m} Tc-piracetam for brain imaging Radiochemistry, 55(6), 624-628 (2013).

[18] Sanad M. H. Novel radiochemical and biological characterization of ^{99m}Tc-

histamine as amodel for brain imaging. J. Anal. Sci. Technol, 5, 23-28 (2014).

[19] Sanad M. H., Emad H. B. Performance characteristics of biodistribution of ^{99m}Tc-cefprozil for in vivo infection imaging. J. Anal. Sci. Technol, 5(1), 1-9 (2014).

[20] Sanad, M.H., Marzook, F.A., Ibrahim, I.T., Abd- Elhaliem, S. M., Farrag, N.S. Preparation and bioevaluation of radioiodinated omberacetam as a radiotracer for brain imaging. Radiochemistry, 65, 114–121 (2023).

[21] Sanad, M.H., Marzook, F.A., Challan, S.A., Essam, H. M., Farrag. A.B. Radioiodination, and Biological Assessment of Olsalazine, as a Highly Selective Radiotracer for Ulcerative Colitis Imaging in Mice. Arab. J. Nucl. Sci. Applications, 56, 105–120 (2023).

[22] Sanad, M.H., Challan, S.A., Essam, H. M., Massoud, A. Assessment of Radiolabeled L-Carnitine for Hepatotoxicity Imaging in Rats. Radiochemistry, 65 (1), 101–113 (2023).

[23] Sanad M.H., Eyssa H.M., Marzook, F.A., Farag, AB., Rizvi, S.F.A., Mandal, S.K. Radioiodinated Procainamide as Radiotracer for Myocardial Perfusion Imaging in Mice. Pharm. Chem J, 57(4), 543–549 (2023).

[24] Sanad, M.H., Eyssa H.M., Marzook, F.A., Farag, AB., et al., Radiocomplexation, Biological Evaluation, and Characterization of [^{99m}Tc]-5-[(3-Carboxy-4-hydroxyphenyl) diazenyl]-2-hydroxybenzoic Acid as a Novel Agent for Imaging of Ulcerative Colitis in Mice. Radiochemistry, 65 (3), 378-386 (2023).

[25] Sanad M. H. Borai E H. Comparative biological evaluation between ^{99m}Tc tricabonyl and ^{99m}Tc-Sn (II) levosalbutamol as a β2-adrenoceptor agonist. Radiochim. Acta, 103, 879-891 (2015).

[26] Sanad M. H. Ibrahim I. T. Radiodiagnosis of Peptic Ulcer with Technetium-99m Labeled Rabeprazole. Radiochemistry, 57(4), 425-430 (2015).

[27] Sanad, M. H., Abelrahman, M. A., Marzook, F. M. A. Radioiodination and biological evaluation of levalbuterol as a new selective radiotracer: a β2-adrenoceptor agonist. Radiochimic. Acta, 104(5), 345-353 (2016).

[28] Borai E. H., Sanad M. H., Fouzy A. S. M. Optimized chromatographic separation and biological evaluation of ^{99m}Tc-clarithromycin for infective inflammation diagnosis. Radiochemistry, 58, 84-91 (2016).

[29] Moustapha, M. E., Motaleb, M. A., Sanad, M. H. Synthesis and biological evaluation of 99mTc-labetalol for β1-adrenoceptor-mediated cardiac imaging. J. Radioanal. Nucl. Chem, 309(2), 511-516 (2016).

[30] Motaleb M. A., Adli, A. S. A., El-Tawoosy M., Sanad M. H., Abd Allah M. An easy and effective method for synthesis and radiolabelling of risedronate as a model for bone imaging. J. Label. Compd. Radiopharm, 59, 157-163 (2016).

[31] Sanad, M.H., Sallam, K., M., Marzook F.A., Abd-Elhaliem S. M. Radioiodination and biological evaluation of candesartan as a tracer for cardiovascular disorder detection J. Label. Compd. Radiopharm, 59, 484-491(2016).

[32] Sanad, M. H., Saad M. M, Fouzy A. S. M., Marzook F., Ibrahim I.T. Radiochemical and biological evaluation of ^{99m}Tc-Labeling of phthalic acid using ^{99m}Tc-Tricabonyl and ^{99m}Tc-Sn (II) as a model for potential hazards imaging. J. Mol. Imag. Dynamic, 6, 1 (2016)

[33] Sanad, M., Farag, A., Husseiny, D. Radioiodination, molecular modelling and biological evaluation of aniracetam as a tracer for brain imaging. E. J. Rad. Sci. Appl, 30(2), 131-143(2017).

[34] Sanad, M. H., Talaat, H. M. Radiodiagnosis of peptic ulcer with technetium-^{99m}-labeled esomeprazole. Radiochemistry, 59(4), 396-401 (2017).

[35] Sanad M. H., Marzook E.A., El-Kawy, O.A. Radiochemical and biological characterization of ^{99m}Tc-oxiracetam as a model for brain imaging. Radiochemistry, 59 (6), 624-629. (2017).

[36] Sanad, M. H., Sakr, T. M., Abdel-Hamid, W. H., Marzook, E. A. In silico study and biological evaluation of 99mTc-tricabonyl oxiracetam as a selective imaging probe for AMPA receptors. J. Radioanal. Nucl. Chem, 314(3), 1505-1515 (2017).

[37] Sanad, M. H., El-Bayoumy, A. S. A., Ibrahim, A. A. Comparative biological evaluation between 99mTc (CO) 3 and 99mTc-Sn (II) complexes of novel quinoline derivative: a promising infection radiotracer. J. Radioanal. Nucl. Chem, 311(1), 1-14 (2017).

[38] Sanad, M. H., Salama, D. H., Marzook, F. A. Radioiodinated famotidine as a new highly selective radiotracer for peptic ulcer disorder detection, diagnostic nuclear

imaging and biodistribution. Radiochimic. Acta, 105(5), 389-398 (2017).

[39] Sanad, M. H., Farag, A. B., Salama, D. H. Radioiodination and bioevaluation of rolipram as a tracer for brain imaging: in silico study, molecular modeling and gamma scintigraphy. J. Label Compd. Radiopharm, 61(6), 501-508 (2018).

[40] Sanad, M. H., Saleh, G. M., Marzook, F. A. Radioiodination and biological evaluation of nizatidine as a new highly selective radiotracer for peptic ulcer disorder detection. J. Label. Compd. Radiopharm, 60(13), 600-607 (2017).

[41] Sanad, M. H., Marzook, E. A., Challan, S. B. Radioiodination of olmesartanmedoxomil and biological evaluation of the product as a tracer for cardiac imaging. Radiochimic. Acta, 106(4), 329-336 (2018).

[42] Sakr, T. M., Sanad, M. H., Abd-Alla, W. H., Salama, D. H., Saleh, G. M. Radioiodinated esmolol as a highly selective radiotracer for myocardial perfusion imaging: In silico study and preclinical evaluation. Appl. Rad. Isot, 137, 41-49 (2018)

[43] Sanad, M. H., Farag, A. B., Saleh, G. M. Radiosynthesis and biological evaluation of 188Re-5, 10, 15, 20-Tetra (4-pyridyl)-21H, 23H-porphyrin complex as a tumor-targeting agent. Radiochemistry, 61(3), 347-351 (2019).

[44] Sanad, M. H., Rizvi, F. A., Kumar, R. R., Ibrahim, A. A. Synthesis and preliminary biological evaluation of 99mTc tricarbonyl ropinirole as apotential brain imaging agent. Radiochemistry, 61(6), 754-758 (2019).

[45] Sanad, M. H., Farag, A. B., Marzook, F. A., Mandal, S K. Radiocomplexation, Chromatographic Separation and Bioevaluation of [99mTc] Dithiocarbamate of Procainamide as Selective Labeled Compound for Myocardial Perfusion Imaging. Pharm. Chem. J, 56(6), 777-784 (2022).

[46] Sanad, M. H., Rizvi, F. A., Kumar, R. R. Radiosynthesis and bioevaluation of ranitidine as highly selective radiotracer for peptic ulcer disorder detection. Radiochemistry, 62(1), 119-124 (2020).

[47] Sanad, M. H., Fouzy, A. S. M., Sobhy, H. M., Hathout, A. S., Hussain, O. A. Tracing the protective activity of Lactobacillus plantarum using technetium-^{99m}-labeled zearalenone for organ toxicity. Int. J. Rad. Biology, 94(12), 1151-1158 (2018).

[48] Sanad, M. H., El-Tawoosy, M., Ibrahim, I. T. Preparation and biological evaluation of 99mTc-Timonacic acid as a new complex for hepatobiliary imaging. Radiochemistry, 59(1), 92-97 (2017).

[49] Sanad M. H., Challan S. B. Radioiodination and biological evaluation of rabeprazole as a peptic ulcer localization radiotracer. Radiochemistry, 59, 307–312 (2017).

[50] Ibrahim, I. T., Abdelhalim, S. M., Sanad, M. H., Motaleb, M. A. (Radioiodination of 3-Amino-2-quinoxalinecarbonitrile 1, 4-Dioxide and its biological distribution in erhlich ascites cancer bearing mice as a preclinical tumor imaging agent. Radiochemistry, 59(3), 301-306 (2017).

[51] Motaleb, M. A., Selim, A. A., El-Tawoosy, M., Sanad, M. H., El-Hashash, M. A. Synthesis, radiolabeling and biological distribution of a new dioxime derivative as a potential tumor imaging agent. J. Rad. Nucl. Chem, 314(3), 1517-1522 (2017).

[52] Sanad, M. H., Sallam, K. M., Salama, D. H. ^{99m}Tc-Oxiracetam as a potential agent for diagnostic imaging of brain: labeling, characterization, and biological evaluation. Radiochemistry, 60(1), 58-63 (2018).

[53] Sanad, M. H., Talaat, H. M., Ibrahim, I. T., Saleh, G. M., Abouzeid, L. A. Radioiodinated celiprolol as a new highly selective radiotracer for β1-adrenoceptor-myocardial perfusion imaging. Radiochimica. Acta, 106(9), 751-757 (2018).

[54] Motaleb, M. A., Sanad, M. H., Selim, A. A., El-Tawoosy, M., Abd-Allah, M. Synthesis, characterization, and radiolabeling of heterocyclic bisphosphonate derivative as a potential agent for bone imaging. Radiochemistry, 60(2), 201-207 (2018).

[55] Motaleb, M. A., Selim, A. A., El-Tawoosy, M., Sanad, M. H., El-Hashash, M. A. Synthesis, characterization, radiolabeling and biodistribution of a novel cyclohexane dioxime derivative as a potential candidate for tumor imaging. Int. j. rad. biology, 94(6), 590-596 (2018).

[56] Sanad M. H., Rizvi S. F. A., Farag A. B. Radiosynthesis and in silico bioevaluation of 131I-Sulfasalazine as a highly selective radiotracer for imaging of ulcerative colitis. Chem. Biol. Drug. Des, 98(5), 751-761 (2021).

[57] Sanad, M. H., Gomaa, N. M., El Bakary, N. M., Ibrahim, I. T., Massoud, A. M. Radioiodination of balsalazide, bioevaluation, and characterization as a

highly selective radiotracer for imaging of ulcerative colitis in mice. Journal of Label. Comp. Radiopharmaceuticals. 65(3), 71-82 (2022).

[58] Sanad, M. H., Ibrahim, A. A., Talaat, H. M. Synthesis, bioevaluation and gamma scintigraphy of Sup.99mTc-N-2-(furylmethyl iminodiacetic acid) complex as a new renal radiopharmaceutical. J. Radioanal. Nucl. Chem., 315(1):57-63 (2018).

[59] Sanad, H. M., Ibrahim, A. A. Radioiodination, diagnostic nuclear imaging and bioevaluation of olmesartan as a tracer for cardiac imaging. Radiochimica Acta, 106(10), 843-850 (2018).

[60] Sanad, M. H., Farag, A. B., Motaleb, M. A. Radioiodination and biological evaluation of landiolol as a tracer for myocardial perfusion imaging: preclinical evaluation and diagnostic nuclear imaging. Radiochimica. Acta, 106(12), 1001-1008 (2018).

[61] Sanad, M. H., Eyssa, H. M., Gomaa, N. M., Marzook, F. A., Bassem, S. A. Radioiodinated esomeprazole as a model for peptic ulcer localization. Radiochimica. Acta. 109(9), 711-718 (2021).

[62] Sanad, M. H., Rizvi, S. F. A., Farrag, A. B. Design of novel radiotracer ^{99m}TcN-tetrathiocarbamate as SPECT imaging agent: a preclinical study for GFR renal function. Chemical Papers, 76(2), 1253-1263 (2022).

[63] Sanad, M. H., Farag, A. B., Marzook, F. A., Mandal, S. K. Preparation, characterization, and bioevaluation of 99mTc-famotidine as a selective radiotracer for peptic ulcer disorder detection in mice. Radiochimica. Acta, 110(1), 67-74 (2022).

[64] Sanad, M. H., Challan, S. B., Marzook, F. A., Abd-Elhaliem, S. M., Marzook, E. A. Radioiodination and biological evaluation of cimetidine as a new highly selective radiotracer for peptic ulcer disorder detection. Radiochimica. Acta, 109(2), 109-117 (2021).

[65] Zvejniece, L., Svalbe, B., Vavers, E., Makrecka-Kuka, M., Makarova, E., Liepins, V., et al. S-phenylpiracetam, a selective DAT inhibitor, reduces body weight gain without influencing locomotor activity". Pharmacology, Biochemistry, and Behavior. 160, 21–29. (2017).

[66] Sanad, M. H., Farag, A. B., Rizvi, S. F. A. In silico and in vivo study of radio-iodinated nefiracetam as a radiotracer for brain imaging in mice. Radiochimica Acta.; 109(7), 575-582 (2021).

[67] Rizvi, S. F. A., Zhang, H., Mehmood, S., Sanad, M. H. Synthesis of ^{99m}Tc-labeled 2-Mercaptobenzimidazole as a novel radiotracer to diagnose tumor hypoxia. Translational oncology, 13(12), 100854 (2020).

[68] Sanad, M. H., Gizawy, M. A., Motaleb, M. A., Ibrahim, I. T., Saad, E. A. A comparative study of stannous chloride and sodium borohydride as reducing agents for the radiolabeling of 2,3,7,8,12,13,17,18-Octaethyl-21H,23H-Porphine with Technetium-^{99m} for tumor imaging. Radiochemistry, 63(4), 512-519 (2021).

[69] Sanad, M. H., Marzook, F. A., Rizvi, S. F. A., Farag, A. B., Fouzy, A. S. M. Radioiodinated azilsartan as a new highly selective radiotracer for myocardial perfusion imaging. Radiochemistry, 63(4), 520-525 (2021).

[70] Sanad, M. H., Abdel Rahim, E. A., Rashed, M. M., Fouzy, A. S. M., Omaima, A. H., Marzook, F. A., Abd-Elhaliem, S. M. (2020): Radioiodination and biological evaluation of parathion as a new radiotracer to study in experimental mice. W. J. Pharmacy. Pharm. Sci, 9(8): 148-158 (2020).

[71] Sanad, M. H., Borai, E. H., Fouzy, A. S. M., Chromatographic separation and utilization of labeled ^{99m}Tc-valsartan for cardiac imaging J. Mol. Imag. Dynamic 4 (1), 1-4 (2014).

[72] Sanad, M. H., HA Shweeta, H. A. Preparation and bio-evaluation of ^{99m}Tc-carbonyl complex of ursodeoxycholic acid for heptobiliary imaging. J. Mol. Imag. Dynamic, 5(1) (2015).

[73] Sanad M. H. Labeling and biological evaluation of ^{99m}Tc-azithromycin for infective inflammation diagnosis. Radiochemistry, 55 (5), 539-544 (2013).

[74] Sanad M. H. Labeling of omeprazole with technetium-^{99m} for diagnosis of stomach. Radiochemistry, 55(6), 605-609 (2013).

[75] Sanad M. H., Abdel-Ghaney, I.Y. Labeling of omeprazole with technetium-99m for diagnosis of stomach. Radiochemistry, 55(4), 418-422 (2013).

[76] Sanad, M.H., Sallam, K., M., Marzook F.A., Abd-Elhaliem S. M. Radioiodination and biological evaluation of irbesartan as a tracer for cardiac imaging. Radiochimic. Acta, 109(1), 41-46 (2016).

[77] Sanad, M.H., Synthesis and labeling of some organic compounds with one of the most radioactive isotope. Ph. D. Thesis, Chemistry Department, Faculty of Science, Ain-Shams University, Cairo, Egypt (2007).

[78] Sanad, M. H., Sallam, K. M., Marzook F.A., Labeling and biological evaluation of ^{99m}Tc-tricarbonyl-chenodiol for hepatobiliary imaging. Radiochemistry, 59, 525–529 (2017).

[79] Motaleb, M. A., Sanad, M. H., Preparation and quality control of ^{99m}Tc-6-{[2-amino-2-(4-hydroxyphenyl)-acetyl] amino}-3-3 ,dimethyl-7-oxo-4-thia-1-azabicyclo-heptane-2-carboxylic acid complex as a model for detecting sites of infection. Arab. J. Nucl. Sci. Applications, 45(3), 71-78 (2012).

[80] Sanad, M.H., Ulcerative Colitis and Peptic Ulcer Imaging, Germany: LAP LAMBERT Academic Publishing, (2017).

[81] Sanad, M.H., Nuclear Medicine and Brain Imaging, Germany: LAP LAMBERT Academic Publishing, (2017).

[82] Motaleb, M.A., Wanis, K.F., Sanad, M. H. Labeling and Biological Distribution of ^{99m}Tc-DCMA-AP. Arab. J. Nucl. Sci. Applications, 39, 84-91 (2006)

[83] EI-Wetery, A.S.A., Fayz, M.A.A., Sanad, M.H., and EI-Hashash, M.A.M., Study on the Preparation of ^{99m} Tc-N (pyrimidine-2-yl-carbamoyl methyl) Iminodiacetic Acid as a New Complex for Hepatobiliary Imaging Agent. Arab. J. Nucl. Sci. Applications, 40, 109-118 (2007).

[84] Sanad, M.H., Marzook, F. A., Gehan, S., Farag, A. B., Talaat, H.M. Radiolabeling, Preparation, and Bioevaluation of ^{99m}Tc-Azathioprine as a Potential Targeting Agent for Solid Tumor Imaging. Radiochemistry, 61, 478-482 (2019).

[85] Sanad, M.H., Synthesis and labeling of some organic compounds with technetium-^{99m}. MS. C. Thesis, Chemistry Department, Faculty of Science, Zagazig Univ.(Banha Branch), Cairo, Egypt (2004) .

[86] Sanad, M. H., Saleh, G. M., Talaat, H. M., In silico study and preclinical evaluation of radioiodinated procaterol as a potential scintigraphic agent for lung imaging, Egyptian Journal of Radiation Sciences and Applications, 30(2), 117-130 (2017).

[87] Motaleb, M.A., Wanis, K.F., Sanad, M.H., Synthesis, characterization and labeling of 2-{N, N-dicarboxymethyl (aminoacetyl)} aminothiazole with technetium-^{99m}. Arab Journal of Nuclear Sciences and Applications, 38, 145–151 (2005).

[88] Eyssa, H. M., El Refay, H. M., Sanad, M. H. Enhancement of the thermal and physicochemical properties of styrene butadiene rubber composite foam using nanoparticle fillers and electron beam radiation. Radiochimic. Acta, 110(3), 205-218 (2022).

[89] Sanad, M. H., Farag, A. B., Sabry A B., Marzook, F.A. Radioiodination of zearalenone and determination of Lactobacillus plantarum effect of on zearalenone organ distribution: In silico study and preclinical evaluation. Toxicology Reports, 9, 470-479 (2022) .

[90] Sanad, M. H., Eyssa, H. M., Marzook, F. A., et al., Optimized chromatographic separation and bioevalution of radioiodinated ilaprazole as a new labeled compound for peptic ulcer localization in mice. Radiochemistry, 63, 811-819 (2021).

[91] Sanad, M. H., Eyssa, H. M., Marzook, F. A., et al., Synthesis, radiolabeling, and biological evaluation of 99mTc-Tricarbonyl mesalamine as a potential ulcerative colitis imaging agent. Radiochemistry, 63, 842-835 (2021).

[92] Sanad, M. H., Marzook, F. A., Farag, A. B., et al., Preparation, biological evaluation and radiolabeling of [99mTc]-technetium tricarbonyl procainamide as a tracer for heart imaging in mice. Radiochimic. Acta, 110(4), 267-277 (2022).

[93] Rizvi, S.F.A., Tania J., Wajeehah S., Sanad, M. H., Haixia Z. Facile one-pot strategy for radiosynthesis of ^{99m}Tc-Doxycycline to diagnose staphylococcus aureus in infectious animal models. Appl. Biochem. Biotechn, 194, 2672–2683 (2022).

[94] Sanad, M. H., Marzook, F. A., Mandal, S.K.., Baidya, M., Radiocomplexation and biological evaluation of ^{99m}Tc tricarbonyl rabeprazole as a radiotracer for peptic ulcer localization. Radiochemistry, 64, 211-218 (2022).

[95] Sanad, M. H., Eyssa, H. M., Marzook, F. A., Farag, A. B., Preparation and bioevaluation of ^{99m}Tc tricarbonyl omeprazole for gastric ulcer localization in mice .Radiochemistry, 64, 54-61 (2021).

[96] Sanad, M. H., Rizvi, S.F.A., FA Marzook., Farag, A. B., In-Silico Study, Preparation and Biological Evaluation of99 MTC-Mesalamine Complex as Radiotracer for Diagnostics and Monitoring of Ulcerative

Colitis in Mice. Pharm. Chem. J, 56(6), 754-761 (2022).

[97] Eyssa, H. M., Elnaggar, M. Y., Zaky, M. M. Impact of graphene oxide nanoparticles and carbon black on the gamma radiation sensitization of acrylonitrile–butadiene rubber seal materials. Polym. Eng. Sci., 61(11), 2843-2860 (2021).

[98] Eyssa, H. M., El Mogy, S. A., Youssef. H. A. Impact of foaming agent and nanoparticle fillers on the properties of irradiated rubber. Radiochimica Acta 109 (2), 127-142 (2021).

[99] Eyssa, H. M., Sadek, R.F., Mohamed, W.S., Ramadan, W. Structure-property behavior of polyethylene nanocomposites containing Bi_2O_3 and WO_3 as an eco-friendly additive for radiation shielding. Ceram. Int, 49(11), 18442–18454 (2023).

[100] Dastjerdi, R., Montazer, M. A review on the application of inorganic nano-structured materials in the modification of textiles: Focus on anti-microbial properties. Colloid. Surf. B, 79: 5-18 (2010).

[101] Shahid, I., U., Shahid, M., Mohammad, F. Green Chemistry Approaches to Develop Antimicrobial Textiles Based on Sustainable Biopolymers—A Review. Ind. Eng.Chem. Res, 52, 5245- 5260 (2013).

[102] Kanikireddy, V., Varaprasad, K., Jayaramudu, T., Karthikeyan, Ch., Sadiku, R. Carboxymethyl cellulose-based materials for infection control and wound healing, Inter. J. Biol. Macromol. 164, 963–975 (2020).

[103] Abdollahi, M., Damirchi, S., Shafafi, M., Rezaei, M., Ariaii, P. Carboxymethyl cellulose agar biocomposite film activated with summer savory essential oil as an antimicrobial agent, Int. J. Biol. Macromol, 126, 561–568 (2019).

[104] Capanema, N. S. V., Mansur, A. A. P., Jesus, A. C. D., Carvalho, S. M., Oliveira, L. C. D., Mansur, H. S. Superabsorbent crosslinked carboxymethyl cellulose-PEG hydrogels for potential wound dressing applications, Inter. J. Biol. Macromol, 106, 1218-1234 (2018).

[105] Lin, C.C., Anseth, K.S. PEG hydrogels for the controlled release of biomolecules in regenerative medicine, Pharm. Res, 26 (3), 631–643 (2009).

[106] Mahmoud, A., Saied, M. A., Naser, A., Fahmy, A. Preparation and characterization of poly (vinyl alcohol)/Carboxymethyl Cellulose/Acrylamide-based membranes for DMFC applications. Egypt. J. Chem. 66(9), 207 - 213 (2023).

[107] Lee, J.H., Nho, Y.C., Lim, Y.M., Son, T.I. Prevention of Surgical Adhesions with Barriers of Carboxymethylcellulose and Poly (ethylene glycol) Hydrogels Synthesized by Irradiation, J. Appl.Polym. Sci, 96, 1138–1145 (2005).

[108] El-Naggar, W. M., Zohdy, M. H., Said, H. M., El-Din, M. S., Noval, D. M. Pigment colors printing on cotton fabrics by surface coating induced by electron beam and thermal curing, Appl. Surf. Sci, 241, 420–430 (2005).

[109] Elmaaty, T. A., Okubayashi, S., Elsisi, H., Abouelenin, S. Electron beam irradiation treatment of textiles materials: a review, J. Polym. Res. 29, 117 (2022).

[110] Thite A.G., Krishnanand K., Sharma D.K., & Mukhopadhyay A.K. Multifunctional finishing of cotton fabric by electron beam radiation synthesized silver nanoparticles. Rad. Phys. Chem, 153, 173–179 (2018).

[111] Khafaga, M. R., Ali H. E., El-Naggar, W. M. Antimicrobial finishing of cotton fabrics based on gamma irradiated carboxymethyl cellulose/poly(vinyl alcohol)/TiO2 nanocomposites, J. Text. Instit, (2015). http://dx.doi.org/10.1080/00405000.2015.1061762

[112] Saleh S. N., Khaffaga, M. M., Ali, N. M., Hassan, M. S., El-Naggar, W. M., Rabie, G. M. Antibacterial functionalization of cotton and cotton/polyester fabrics applying hybrid coating of copper/chitosan nanocomposites loaded polymer blends via gamma irradiation, Inter. J. Biolog. Macromol, 183, 23–34 (2021).

[113] Leone, A., Spada, A., Battezzati, A., Schiraldi, A., Aristil, J., Bertoli, S. Cultivation, genetic, ethnopharmacology, phytochemistry and pharmacology of *Moringa oleifera leaves*: an overview. Int. J. Molec. Sci, 16, 12791 (2015b).

[114] Amin, A. A., Soliman, H. A., Hashem, K. S. Survival, Growth, Haematological and Biochemical Responses of Clarias Gariepinus Grown in Moringa Oleifera Seeds Treated Wastewater. Egypt. J. Chem. 67(3), 1-11 (2024).

[115] Eyssa, H.M., Sawires, S.G., Senna, M.M. Gamma Irradiation of Polyethylene Nanocomposites for Food Packaging Applications against Stored-Product Insect Pests. J. Vinyl. Add. Tech, 25, 120-129 (2019).

[116] Selvarani, T., Prabhu B., Thenmozhi, K. Effect of aqueous extract from the sea weed, Sargassum illicifolium, on three types of non-pathogenic terrestrial bacteria. Inter. J. Medic & Arom. Plant, 3(2), 169-177 (2013).

[117] El Sayed, A. M., El-Gamal, S., Morsi, W. M., Mohammed, Gh. Effect of PVA and copper oxide nanoparticles on the structural, optical, and electrical properties of carboxymethyl cellulose films, J. Mater. Sci, 50, 4717–4728 (2015).

[118] Jassim, S. H., Salman, T. A. The Potential of Green-Synthesized Copper Oxide Nanoparticles from Coffee Aqueous Extract to Inhibit Testosterone Hormones. Eypt. J. Chem. 65(4), 395 – 402 (2022).

[119] Shammout, M. W., Awwad, A. M. A novel route for the synthesis of copper oxide nanoparticles using Bougainvillea plant flowers extract and antifungal activity evaluation, Chem. Int, 7(1), 71-78 (2021).

[120] Sharma, S., Kumar, K., Thakur, N., Chauhan, S., Chauhan, M. S. Eco-friendly Ocimum tenuiflorum green route synthesis of CuO nanoparticles: Characterizations on photocatalytic and antibacterial activities, J. Enviro. Chem. Eng, 9, 105395 (2021).

[121] Liang, C. Y., Marchessault, R.H. Infrared spectra of crystalline polysaccharides. II. Native celluloses in celluloses in the region from 640 to 1700 cm-1. J. Polym. Sci, X, 269-278 (1959).

[122] Bozaci, E., Akar, E., Ozdogan, E., Demir, A., Altinisik, A., Seki, Y. Application of carboxymethylcellulose hydrogel based silver nanocomposites on cotton fabrics for antibacterial property, Carbohyd. Polym, (2015).http://dx.doi.org/10.1016/j.carbpol.2015.07.036.

[123] Kono, H. Characterization and properties of carboxymethyl cellulose hydrogels crosslinked by polyethylene glycol, Carboh. Polym, 106, 84–93 (2014).

[124] Adebajo, M.O., Frost, R.L. Acetylation of Raw Cotton for Oil Spill Cleanup Application - An FTIR and 13C MAS NMR Spectroscopic Investigation. Spectrochim. Act, P. A: Molecul & Biomol. Spectro, 60(10), 2315-2321 (2004).

[125] Shankar, S., Wang, L.F., Rhim, J.W. Preparation and properties of carbohydrate-based composite films incorporated with CuO nanoparticles, Carbohy. Polym, 169, 264–271 (2017).

[126] Chen, W., Chen, J., Feng, Y. B., Hong, L., Chen, Q.Y., Wu, L.F., Lin, X.H., Xia, X.H. Peroxidase-like activity of water-soluble cupric oxide nanoparticles and its analytical application for detection of hydrogen peroxide and glucose. Analyst, 137, 1706–1712 (2012).

[127] Ibarra, L., Rodríguez, A., Barrantes, I. M. Crosslinking of carboxylated nitrile rubber (XNBR) induced by coordination with anhydrous copper sulfate), Polym. Int. 58: 218-226 (2009).

[128] Chambi, H., Grosso, C. Edible films produced with gelatin and casein cross-linked with transglutaminase, Food. Res. Int, 39, 458–466 (2006).

[129] Al-Muhtaseb, A. H., Mcminn, W. A. M., Mage, T. R. A. Moisture Sorption Isotherm Characteristics of Food Products: A Review, Food. Biopro. Proc, 80, 118-128 (2002).

[130] Li, N. Zeng, F., Wang, Y., Qu, D., Hu, W., Luan, Y., Dong, S., Zhangd, J., Bai, Y. Fluorinated polyurethane based on liquid fluorine elastomer (LFH) synthesis via two-step method: The critical value of thermal resistance and mechanical properties. RSC. Adv, 7 30970 (2017).

[131] Shin, J.Y., Lee, D. Y., Kim, B.Y., Yoon, J. I. Effect of polyethylene glycol molecular weight on cell growth behavior of polyvinyl alcohol/carboxymethyl cellulose/polyethylene glycol hydrogel, J Appl Polym Sci, 137, e49568 (2020).

[132] Manikandan, A., Sathiyabama, M. Green Synthesis of Copper-Chitosan Nanoparticles and Study of its Antibacterial Activity, Nanomedic & Nanotech. 6, 2–5 (2015).

[133] Bogdanovic, U., Vodnik, V., Mitric, M., Dimitrijevic, S., Skapin, S. D. V., Budimir, Z. M., M. Stoiljkovic Nanomaterial with High Antimicrobial Efficacy Copper/Polyaniline Nanocomposite. ACS appl. mater & int, 7(3), 1955-1966 (2015).

[134] Cioffi, N. L., Torsi, N., Ditaranto, G., Tantillo, L., Ghibelli, L., Sabbatini, T., Bleve-Zacheo, M., D'Alessio, P. G., Traversa, Z. E. Copper nanoparticle/polymer composites with antifungal and bacteriostatic properties. Chemistry of Materials 17(21): 5255-5262 (2005).